

New light on the search for low metallicity galaxies

I. The N2 calibrator

Glenda Denicoló¹, Roberto Terlevich^{1*} and Elena Terlevich,^{2†}

¹*Institute of Astronomy, Madingley Road, Cambridge, CB3 0HA, United Kingdom*

²*Instituto Nacional de Astrofísica, Óptica y Electrónica, Tonantzintla, Puebla, Mexico*

25 October 2018

ABSTRACT

We present a simple metallicity estimator based on the logarithmic $[\text{N II}] \lambda 6584\text{\AA}/\text{H}\alpha$ ratio, hereafter N2, which we envisage will become very useful for ranking galaxies in a metallicity sequence from redshift survey quality data even for moderately low spectral resolution.

We have calibrated the N2 estimator using a compilation of H II galaxies having accurate oxygen abundances, plus photoionization models covering a wide range of abundances. The comparison of models and observations indicates that both primary and secondary nitrogen are important for the relevant range of metallicities.

The N2 estimator follows a linear relation with $\log(\text{O}/\text{H})$ that holds for the whole abundance range covered by the sample, from about 1/50th to twice the Solar value ($7.2 < 12 + \log(\text{O}/\text{H}) < 9.1$). We suggest that the $([\text{S II}] \lambda\lambda 6717, 6731\text{\AA}/\text{H}\alpha)$ ratio (hereafter S2) can also be used as a rough metallicity indicator. Because of its large scatter the S2 estimator will be useful only in systems with very low metallicity, where $[\text{N II}] \lambda 6584\text{\AA}$ is not detected or in low resolution spectra where $[\text{N II}] \lambda 6584\text{\AA}$ is blended with $\text{H}\alpha$.

Key words: galaxies: abundances – galaxies: stellar content – galaxies: evolution

1 INTRODUCTION

The key for accurate determination of oxygen abundance in gaseous ionized nebulae is a precise measurement of the weak auroral forbidden emission line $[\text{O III}] \lambda 4363\text{\AA}$. In narrow emission line starforming galaxies the temperature sensitive $[\text{O III}] \lambda 4363\text{\AA}$ line intensity correlates with the overall abundance, being relatively strong in very low metallicity systems ($12 + \log(\text{O}/\text{H}) < 7.8$) and becoming undetectable even for moderately low metallicity galaxies ($12 + \log(\text{O}/\text{H}) > 8.3$). As a result, for most of the starforming galaxies $[\text{O III}] \lambda 4363\text{\AA}$ is unmeasurably weak.

For the large majority of starforming regions the oxygen abundance is therefore estimated using empirical methods based on the relative intensities of strong, easily observable, optical lines. Although abundances derived in this way are recognized to suffer considerable uncertainties, still they are believed to be able to roughly trace general trends in galaxies. The most widely used empirical abundance calibrators are the R_{23} (Pagel *et al.* 1979) and, recently, the $S_{23(4)}$ (Vílchez & Esteban 1996; Díaz & Pérez-Montero 2000; Oey & Shields 2000) parameters.

The R_{23} method was first proposed by Pagel *et al.* (1979) and subsequently developed and calibrated by many authors (Edmunds & Pagel 1984, McCall, Rybski & Shields 1985, Dopita & Evans 1986, Torres-Peimbert, Peimbert & Fierro 1989, McGaugh 1991). It is defined as the sum of the flux of $[\text{O II}] \lambda 3727\text{\AA}$ and $[\text{O III}] \lambda\lambda 4959, 5007\text{\AA}$ lines relative to $\text{H}\beta$ ($R_{23} = ([\text{O II}] \lambda 3727\text{\AA} + [\text{O III}] \lambda\lambda 4959, 5007\text{\AA})/\text{H}\beta$). The R_{23} method can be used to estimate abundances up to relatively high redshifts, but there are a few problems associated with the use of this estimator. Firstly, it is bi-valued, i.e. a single value of R_{23} can be due to two very different oxygen abundances. Secondly, a very large fraction of the starforming regions lie on the ill-defined turning zone around $12 + \log(\text{O}/\text{H}) \simeq 8.1$ where regions with the same R_{23} value have oxygen abundances which differ by almost an order of magnitude. Thirdly, the R_{23} method requires spectrophotometric data and given the wavelength range covered, the reddening correction of the lines involved becomes crucial. Finally a characteristic which is readily apparent is the large scatter in the R_{23} vs. oxygen abundance calibration, larger than accounted for by observational errors (Kobulnicky, Kennicutt & Pizagno 1999).

The S_{23} parameter introduced by Vílchez & Esteban (1996) is defined as the sum of the flux of $[\text{S II}] \lambda\lambda 6717, 6731\text{\AA}$ and $[\text{S III}] \lambda\lambda 9069, 9532\text{\AA}$ relative to $\text{H}\beta$ (S_{23}

* Visiting Professor, INAOE, Puebla, Mexico

† Visiting Fellow, IoA, Cambridge

$= ([\text{S II}] \lambda\lambda 6717, 6731\text{\AA} + [\text{S III}] \lambda\lambda 9069, 9532\text{\AA})/H\beta$). Unlike the R_{23} method, the relation between S_{23} and oxygen abundance remains single valued up to a metallicity slightly higher than solar. Díaz & Pérez-Montero (2000, hereafter DP00) show an empirical calibration of the S_{23} parameter with a somewhat reduced scatter as compared to that with R_{23} . This calibration should be improved by the inclusion of high quality data at both the low and the high metallicity ends, but otherwise looks very promising for metallicities up to solar. On the other hand, Oey & Shields (2000) argued that the S_{23} method is more sensitive to the ionization parameter than R_{23} , and propose to include the emission of $[\text{S IV}]$ to overcome the limitations of S_{23} , introducing the S_{234} method. A problem with this estimator is that good data is still scarce, and that the detection of the sulphur lines in the near-infrared is limited to galaxies with redshifts smaller than about 0.1.

In all, the estimation of abundances of large number of galaxies, particularly in the slightly subsolar to oversolar range, is still a difficult problem. This metallicity regime contains most of the H II regions in early spiral galaxies and the inner regions of most late type galaxies, therefore the description of the metallicity distribution in galaxies cannot be complete without it.

Storchi-Bergmann *et al.* (1994) suggested the use of $N2 = [\text{N II}] \lambda 6584\text{\AA}/H\alpha$, as an abundance estimator. Their calibration of the $N2$ vs. O/H relation was improved by Raimann *et al.* (2000) that proposed a new calibration using the Terlevich *et al.* (1991, hereafter T91) sample.

In the present work we have used the best available abundance data for starforming galaxies in combination with photoionization models to explore the usefulness of the $N2$ abundance estimator and to calibrate it in terms of metallicity.

The data set is presented in Section 2. The new calibration of the $N2$ estimator with photoionization models is discussed in Sections 3 and 4. The concluding remarks are given in Section 5.

2 THE DATA

We have compiled from the literature a sample with the best available data on the lines of interest.

The published data included in our sample was selected for having high signal-to-noise, spectral resolution better than $\sim 8 \text{\AA}$ in order to separate $[\text{N II}] \lambda 6584\text{\AA}$ from $H\alpha$, easily accessible line strengths and errors. In computing abundances and line ratios, we have adopted the $c(H\beta)$ reddening factor published by the respective authors.

The sample of low metallicity galaxies is based on a compilation by Kobulnicky & Skillman (1996) and is not intended to be complete, but includes the majority of the best spectrophotometric data available for H II galaxies.

The data for the metal-poor galaxy sample (i.e., with available $[\text{O III}] \lambda 4363\text{\AA}$ intensity and $12+\log(O/H) < 8.4$) are presented in Table 1, together with their corresponding observational errors propagated from the emission line uncertainties quoted in the original references. We re-determined the electron temperatures and abundances applying the method and expressions from Section 4 of Pagel *et al.* (1992) to the reddening corrected emission line fluxes. In

Table 1, objects within references 1-17 had their metallicities computed using the $[\text{O III}] \lambda 4363\text{\AA}$ line intensity. Galaxies with more than one H II region may appear more than once in the table. The comparison of the tabulated values can give an idea of observational and systematic errors and possible spatial variations. We have added to the sample from the literature, our measurements of six metal-poor galaxies discovered by us on the Anglo-Australian 4.0m telescope in August 1996 and August 1997 (Terlevich *et al.* 2001, hereafter Paper II). The total number of low metallicity objects with $12+\log(O/H)$ computed using the $[\text{O III}] \lambda 4363\text{\AA}$ line intensity is 108.

The sample of metal-rich galaxies (128) includes data from DP00; Castellanos, Díaz & Terlevich (2001, hereafter CDT01) and T91. For galaxies with weak or none $[\text{O III}] \lambda 4363\text{\AA}$ emission (i.e., $12+\log(O/H) > 8.4$), we derived the metallicity using R_{23} (the *upper* branch analytic expression by McGaugh, published in Kobulnicky *et al.* 1999) or S_{23} (Díaz & Pérez-Montero 2000) methods, depending on the availability of the $[\text{S III}] \lambda\lambda 9069, 9532\text{\AA}$ lines. The errors for the metallicity values derived by the R_{23} parameter already account for the intrinsic 0.2 dex uncertainty of the method. The 55 metal-rich galaxies included in Table 1 with references 18-26 correspond to the compilation in DP00 and to CDT01 and had their metallicities estimated by the R_{23} or S_{23} methods. The rest of the metal rich galaxies, as they are from T91, were not included in the table.

The whole range of oxygen abundances covers from $\sim 2\%$ solar (Solar is taken as $12+\log(O/H)_{\odot} = 8.91$) for IZw18 to more than solar for some regions for which detailed modeling has been performed (see compilation in DP00).

3 RESULTS

The $N2$ parameter is defined as

$$N2 = \log([\text{N II}] \lambda 6584/H\alpha). \quad (1)$$

The relation between $N2$ and the oxygen abundance is shown in Figure 1. It can be seen that these two parameters are well correlated (linear correlation coefficient of 0.85) and that a single slope is capable of describing the whole metallicity range, from the most metal-poor to the most metal-rich galaxies in the sample. The heavy solid line represents the linear fit to the $N2$ vs. $12+\log(O/H)$ relation. Least squares fits to the data simultaneously minimizing the errors in both axes, give

$$12+\log(O/H) = 9.12(\pm 0.05) + 0.73(\pm 0.10) \cdot N2, \quad (2)$$

The thin solid line in Figure 1 shows the linear fit from Raimann *et al.* (2000). Given the differences among our samples and the smaller number of points in Raimann *et al.* data, we conclude that both solutions are in basic agreement. However both fits dramatically disagree with the calibration proposed by Storchi-Bergmann *et al.* (1994, section 4).

3.1 Photoionization models

We have computed a grid of photoionization models using CLOUDY (Ferland 1996) for abundances $[O/H] = 0.04, 0.2, 1$ and 2 . All the elements apart from N are assumed to be

Table 1. Chemical abundances and $[\text{N II}] / \text{H}\alpha$ ratios.

Galaxy	12+log(O/H)	N2	Ref.	Galaxy	12+log(O/H)	N2	Ref.
I Zw 18nw	7.196±0.046	-2.527±0.068	1	1437+370	7.971±0.064	-1.678±0.022	4
I Zw 18se	7.309±0.057	-2.317±0.017	1	Pox 139	7.983±0.083	-1.669±0.123	12
SBS 0335-052W	7.285±0.051	-2.100±0.119	2	UM 462	7.984±0.063	-1.676±0.059	10
UGCA 292-1	7.320±0.050	-1.943±0.046	3	N5253 A	7.991±0.069	-1.106±0.010	10
UGCA 292-2	7.361±0.060	-2.104±0.060	3	N5253-6	8.025±0.066	-1.053±0.020	13
0940+544 N	7.377±0.040	-2.224±0.055	4	N5253-5	8.094±0.067	-1.123±0.021	13
HS 0822+3542	7.395±0.045	-2.260±0.040	5	N5253-1	8.144±0.076	-1.182±0.012	13
1159+545	7.473±0.045	-2.067±0.040	4	N5253-2	8.167±0.072	-1.215±0.021	13
1415+437	7.522±0.047	-1.922±0.014	6	N5253-4	8.180±0.069	-1.179±0.024	13
0832+699	7.587±0.052	-1.982±0.015	4	N5253 B	8.266±0.104	-1.161±0.036	10
T1214-277	7.596±0.052	-2.493±0.048	7	T1304-386	8.001±0.067	-1.508±0.031	10
UGC4483 S	7.601±0.055	-1.982±0.019	8	UM 469	8.001±0.080	-1.181±0.045	10
1211+540	7.687±0.054	-2.142±0.022	4	37-27	8.012±0.064	-1.630±0.025	9
1249+493	7.721±0.053	-1.926±0.054	6	1533+469	8.012±0.062	-1.261±0.011	6
537-69	7.735±0.101	-1.628±0.046	9	Mrk 600	8.019±0.068	-1.873±0.122	7
T1304-353	7.745±0.055	-2.263±0.116	10	1135+581	8.019±0.069	-1.625±0.006	4
70-05b	7.751±0.087	-1.719±0.086	9	Pox 108	8.026±0.089	-1.669±0.123	12
UM 461	7.795±0.057	-2.251±0.022	7	Pox 4 NW	8.031±0.082	-1.675±0.123	12
C1543+091	7.796±0.059	-1.939±0.109	10	0946+558	8.034±0.067	-1.645±0.014	4
1331+493 N	7.819±0.057	-1.940±0.027	4	0948+532	8.039±0.068	-1.617±0.020	4
1331+493 S	7.911±0.062	-1.441±0.031	6	T1345-420	8.049±0.067	-1.716±0.048	10
1152+579	7.850±0.057	-1.844±0.022	4	II Zw 70	8.067±0.090	-1.346±0.029	11
Mrk 36	7.865±0.099	-1.827±0.087	11	T1334-326	8.088±0.072	-1.928±0.106	10
25-10	7.865±0.076	-1.140±0.154	9	II Zw 40	8.104±0.077	-1.708±0.024	10
Pox 120	7.868±0.082	-1.745±0.123	12	II Zw 40	8.183±0.091	-1.778±0.051	11
Mrk 36	7.872±0.064	-1.901±0.100	10	N6822-HuX	8.104±0.086	-1.740±0.100	14
46-17	7.891±0.061	-1.968±0.028	9	T1004-296 SE	8.117±0.072	-1.290±0.020	10
C1148-203	7.896±0.063	-1.775±0.029	10	T1004-296 NW	8.204±0.083	-1.386±0.016	10
Pox 105	7.904±0.081	-1.669±0.123	12	Tol 35	8.121±0.087	-1.547±0.123	12
297-24	7.939±0.081	-1.325±0.083	9	T0633-415	8.144±0.072	-1.373±0.150	10
C0840+120	7.940±0.063	-1.615±0.056	10	T0633-415	8.144±0.071	-1.391±0.008	7
Fairall 30	7.949±0.064	-1.634±0.022	10	Fairall 2	8.169±0.074	-1.155±0.066	10
Tol 2	7.965±0.080	-1.351±0.123	12	T1324-276	8.170±0.077	-1.895±0.024	10

References to the table.

(1)Skillman & Kennicutt 1993; (2)Lipovetsky *et al.* 1999; (3)van Zee 2000; (4)Izotov, Thuan & Lipovetsky 1994; (5)Kniazev *et al.* 2000; (6)Thuan, Izotov & Lipovetsky 1995; (7)Pagel *et al.* 1992; (8)Skillman *et al.* 1994; (9)Terlevich *et al.* 2001; (10)Campbell, Terlevich & Melnick 1986; (11)Garnett 1990; (12)Kunth & Joubert 1985; (13)Walsh & Roy 1989; (14)Pagel, Edmunds & Smith 1980.

primary and are therefore scaled as oxygen. For nitrogen we used $[\text{N}/\text{O}] = 0.08 + [\text{O}/\text{H}]$ that represents a realistic combination of early primary N plus later secondary N and reproduces the observed behaviour of N/O with O/H (Henry, Edmunds & Köppen, 2000 and references therein). The square brackets in the expressions denote the value relative to that of Orion, i.e., N: 7.00×10^{-5} , O: 4.00×10^{-4} . For simplicity we have used single star models with $T_{eff} = 45000$ K. Changing to cluster models or including a metallicity dependent T_{eff} do not change the basic results. The photoionization models are shown as dashed and dot-dashed lines in Figure 1. The lines join models with the same ionization parameter (U). The whole range of the data is comprised between the models with $\log(U) = -1.5$ and $\log(U) = -3.0$. It can be seen that within the errors there is a good superposition between models and observations.

Models with either pure primary or pure secondary nitrogen fail to reproduce the slope of the relation. The change in N2 per unit O/H change is too large when compared with the data, for the pure secondary N models, while it is too small for the pure primary ones.

The abundance parameter N2 vs. the ionization parameter sensitive ratio (for ionizing temperatures higher than about 35000 K) $\log([\text{O II}] / [\text{O III}])$, is shown in Figure 2, together with the photoionization model results. The lines represent again photoionization models with the same ionization parameter and covering the whole range of metallicity. As can be seen, the lines for constant ionization parameter are almost vertical and at a given metallicity the range in N2 covered by changing the ionization parameter is much smaller than the observed range. This confirms that most of the observed trend of N2 with O/H is due to metallicity changes.

4 DISCUSSION

Although relatively tight, the relation between N2 and abundance has a scatter that might be larger than the observational errors.

The comparison of models and data in Figure 2 suggests that some of the scatter in the N2 vs. 12+log(O/H)

Table 1. *continued*

Galaxy	12+log(O/H)	N2	Ref.	Galaxy	12+log(O/H)	N2	Ref.
T1457-262 A	8.170±0.074	-1.362±0.065	10	NGC3310 E	8.482±0.051	-0.687±0.005	21
T1457-262 B	8.230±0.081	-1.666±0.058	10	NGC3310 L	8.551±0.077	-0.563±0.008	21
T1008-286	8.174±0.073	-1.471±0.078	10	NGC3310 M	8.483±0.374	-0.824±0.013	21
UCM1612+1308	8.183±0.070	-1.593±0.012	15	NGC7714 A	8.473±0.051	-0.509±0.011	22
C1409+120	8.186±0.075	-1.301±0.114	10	NGC7714 N110	8.553±0.179	-0.305±0.044	22
N4212 C20	8.192±0.090	-1.093±0.027	16	NGC7714 B	8.280±0.051	-0.873±0.011	22
N4214 A6	8.221±0.077	-1.058±0.027	16	NGC7714 C	8.265±0.167	-0.859±0.070	22
N4214 C6	8.374±0.087	-1.197±0.027	16	NGC7714 N216	8.607±0.199	-0.322±0.036	22
T0440-381	8.212±0.074	-1.447±0.054	10	M101 NGC5471	8.182±0.119	-1.640±0.157	23
Mrk 5	8.214±0.090	-1.309±0.053	11	M101 NGC5471	8.012±0.123	-1.468±0.024	19
LMC II2	8.225±0.084	-1.612±0.061	17	M101 NGC5471A	7.986±0.142	-1.553±0.054	24
Mrk 67	8.226±0.094	-1.721±0.068	11	M101 NGC5471B	8.295±0.146	-1.095±0.019	24
T1116-325	8.336±0.096	-1.537±0.080	10	M101 NGC5471C	8.187±0.179	-0.994±0.030	24
M33 CC93	8.497±0.164	-0.540±0.021	18	M101 NGC5471D	8.200±0.210	-1.553±0.054	24
M33 IC142	8.583±0.142	-0.694±0.031	18	M101 NGC5471E	8.158±0.205	-1.757±0.087	24
M33 NGC595	8.407±0.049	-0.816±0.012	18	M101 NGC5455	8.353±0.235	-0.925±0.026	24
M33 NGC595	8.461±0.188	-0.735±0.029	19	M101 NGC5455	8.480±0.188	-0.771±0.153	23
M33 MA2	8.401±0.073	-1.031±0.033	18	M101 NGC5461	8.499±0.339	-0.854±0.022	24
M33 NGC604	8.414±0.061	-0.902±0.003	18	M51 CCM72	9.095±0.215	-0.493±0.013	25
M33 NGC604	8.260±0.131	-0.940±0.020	19	M51 CCM24	9.040±0.222	-0.464±0.063	25
M33 NGC588	8.348±0.099	-1.553±0.033	18	M51 CCM10	8.973±0.206	-0.413±0.043	25
M33 NGC588	8.395±0.244	-1.346±0.023	19	NGC628 H13	8.194±0.023	-0.761±0.008	26
M33 IC131	8.357±0.263	-0.959±0.026	19	NGC628 H3	8.234±0.024	-0.784±0.024	26
NGC2403 VS35	8.430±0.086	-0.706±0.019	20	NGC628 H4	8.310±0.026	-0.679±0.040	26
NGC2403 VS24	8.423±0.129	-0.828±0.019	20	NGC628 H5	8.340±0.028	-0.678±0.040	26
NGC2403 VS38	8.365±0.150	-0.860±0.019	20	NGC925 CDT1	8.520±0.038	-0.693±0.029	26
NGC2403 VS44	8.332±0.125	-0.876±0.019	20	NGC925 CDT2	8.719±0.051	-0.602±0.037	26
NGC2403 VS51	8.353±0.196	-1.012±0.020	20	NGC925 CDT3	8.505±0.041	-0.639±0.035	26
NGC2403 VS3	8.333±0.192	-0.948±0.019	20	NGC925 CDT4	8.414±0.032	-0.682±0.018	26
NGC2403 VS49	8.362±0.157	-1.106±0.021	20	NGC1232 CDT1	8.440±0.032	-0.441±0.012	26
NGC3310 Nuc	8.831±0.059	-0.298±0.007	21	NGC1232 CDT2	8.597±0.041	-0.602±0.024	26
NGC3310 A	8.212±0.023	-0.797±0.003	21	NGC1232 CDT3	8.519±0.037	-0.508±0.027	26
NGC3310 B	8.441±0.032	-0.638±0.007	21	NGC1232 CDT4	8.516±0.037	-0.578±0.023	26
NGC3310 C	8.482±0.035	-0.719±0.003	21	NGC1637 CDT1	8.226±0.024	-0.438±0.026	26

References to the table.

(10)Campbell, Terlevich & Melnick 1986; (11)Garnett 1990; (15)Rego *et al.* 1998; (16)Kobulnicky & Skillman 1996; (17)Mathis, Chu & Peterson 1985; (18)Vílchez *et al.* 1988; (19)Garnett 1989; (20)Garnett *et al.* 1997; (21)Pastoriza *et al.* 1993; (22)González-Delgado *et al.* 1994; (23)Shields & Searle 1978; (24)Kennicutt & Garnett 1996; (25)Díaz *et al.* 1991; (26)Castellanos, Díaz & Terlevich 2001.

relation could in principle depend on the degree of ionization of the nebula that in turn may depend on the age of the ionizing cluster. To cover the whole data range in the N2 vs. O/H relation, it was needed to vary the ionization parameter U from $\log(U)=-3$ to -1.5 , with a best fit corresponding to $\log(U) \cong -2$.

In an attempt to understand the dispersion in the O/H – N2 relation, we have studied the connection between the scatter of the N2 parameter and an age sensitive parameter, the equivalent width of $H\beta$, $EW(H\beta)$. The ranking of $EW(H\beta)$ with age (Copetti, Pastoriza & Dottori, 1986; Leitherer & Heckman 1995) goes in the sense that $EW(H\beta)$ in emission reaches values of several hundred Å for an H II region photoionized by a zero-age coeval stellar population and decreases as the cluster evolves and the stellar age increases. No significant trend was found between these two variables for the bulk of our sample, but a clear trend is visible for those with the highest quality $EW(H\beta)$ and O/H determinations. This result suggests that the presence of a range of ages in the data may be responsible for part of the scatter in the N2 vs. O/H diagram. This trend is shown in

Figure 3 where we plotted the distance to the regression line in Figure 1 versus the $EW(H\beta)$. There is a clear trend suggesting that part of the scatter is correlated with $EW(H\beta)$. Intrinsic variations in the N/O abundance ratio will of course constitute another source of scatter.

We can also expect dispersions of the order of 0.05-0.2 dex in metallicity due to the differences between global spectra and smaller aperture exposures (Kobulnicky, Kennicutt & Pizagno 1999). This difference becomes more important when comparing low redshift galaxies with high- z spatially integrated spectra. Several effects may cause the emission-line ratios to produce oxygen abundance estimates significantly lower than those derived from small aperture observations of individual H II regions. Kobulnicky *et al.* (1999) demonstrated through simple modeling, that temperature fluctuations are the primary cause for overestimating the electron temperature and underestimating the oxygen abundance, and that ionization parameter variations further exacerbate this systematic underestimation. We therefore consider our emission line measurements and abundance determinations from global spectra as lower limits. A more careful analysis

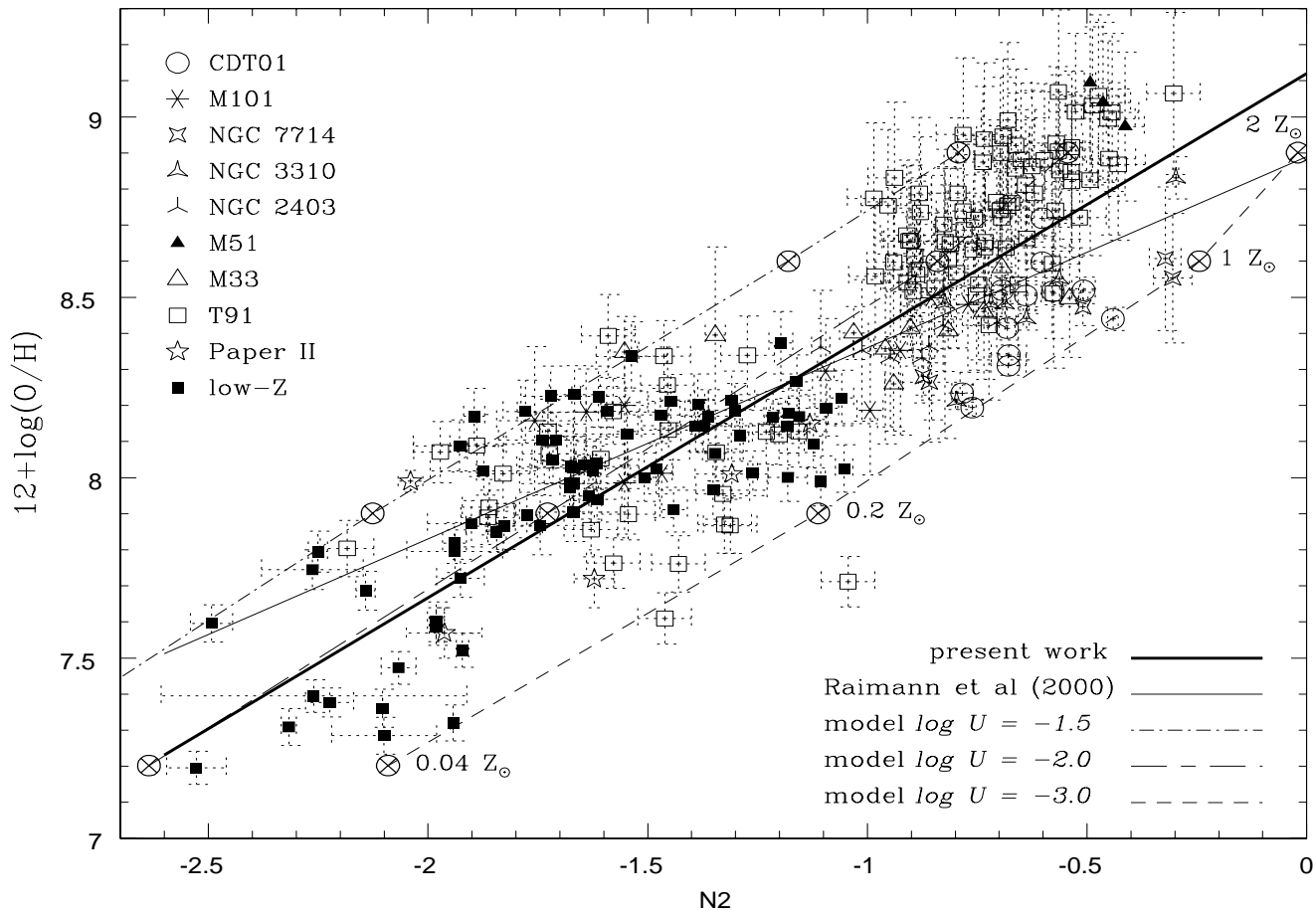


Figure 1. Oxygen abundance vs. the N2 calibrator (see text) for the whole dataset. The linear fit to the data, heavy solid line, taking into account the dispersion in the distribution, gives $12+\log(\text{O}/\text{H}) = 9.12+0.73\cdot\text{N}2$, with a correlation coefficient of 0.85. The crossed-circle dots correspond to the photoionization model points for the metallicities as labelled by the side of the dots. The symbols refer to the galaxies in Castellanos, Díaz & Terlevich 2001 (CDT01); six metal-poor galaxies from Terlevich *et al.* 2001 (Paper II), and a selected sample of low metallicity galaxies with references in Table 1. The only galaxies not listed in Table 1 come from the catalogue of H II galaxies of Terlevich *et al.* 1991 (T91).

of spatial variation effects on emission line intensities will be carried out in Paper II.

The N2 parameter has clear observational advantages for ranking metallicities in starforming galaxies. Besides it being single-valued, it also appears to have a tighter correlation with O/H than R₂₃; still, it has the drawback of using forbidden lines of N, making the abundance calibrator sensitive to variations on the N/O abundance ratio. Photoionization models taking into account *primary plus secondary* nitrogen encompass the data in the N2 vs. 12+log(O/H) plane. To reproduce the dispersion it is enough to vary the ionization parameter U in the models by (+0.5,-1.0), with an average fit of $\log(U) \cong -2.0$.

We can expect that for the very low metallicity galaxies, the nitrogen lines would become less sensitive to metallicity due to the increasing presence of primary N in comparison to secondary N. Although we do not clearly see this behavior in our sample, we find that an alternative line ratio for the low metallicity branch would be useful, as the [N II] lines also become too faint and difficult to deblend from H α once in this regime. We adopted the ratio $\log([\text{S II}] \lambda\lambda 6717,6731\text{\AA}/\text{H}\alpha)$ (S2) as an alternative. In Figure 4 we show the relation of S2

with metallicity. This relation still has the advantage of not being strongly dependent on reddening corrections, but its scatter is apparently larger than for the N2 – 12+log(O/H) relation.

We emphasize that the N2 relation is clearly not better than the S₂₃₍₄₎ methods, although it is observationally much easier to obtain, specially for moderate redshift objects. It therefore has the advantage of allowing a very fast ranking of galaxies in a metallicity sequence, in particular when searching for low metallicity objects. A test for this method was performed on the Durham redshift survey data and is the subject of Paper II.

5 CONCLUSIONS

We have collected from the literature a representative sample of spectroscopic measurements of starforming galaxies covering a wide range in metallicity ($7.2 \lesssim 12+\log(\text{O}/\text{H}) \lesssim 9.1$), and recalculated oxygen abundances in a self-consistent manner. We confirmed previously published results on the correlation between the logarithmic ratio of

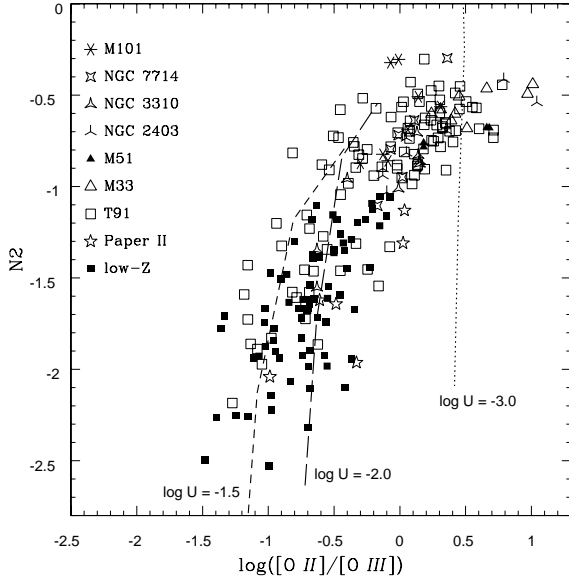


Figure 2. The N2 parameter plotted against the ionization sensitive parameter $\log([O II]/[O III])$. The lines join models with the same ionization parameter for abundances $[O/H] = 0.04, 0.2, 1, 2 Z_{\odot}$.

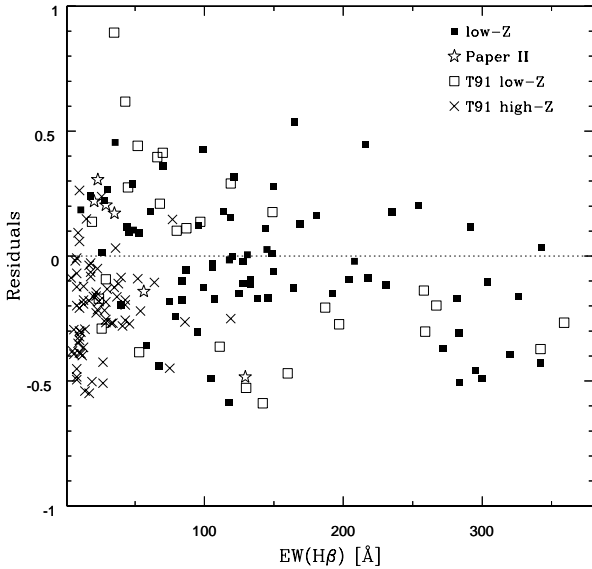


Figure 3. Residuals of the linear regression shown in Figure 1 against equivalent width of $H\beta$. The low metallicity sample can be found in Table 1.

$[N II]/H\alpha$ (N2) and O/H and obtained an improved calibrator thanks to a larger sample of carefully and consistently calculated abundances and line ratios.

Considering the weak points and limitations of empirical abundance determination methods, we reckon that using N2 as a metallicity calibrator presents several advantages: it involves easily measurable lines that are available for a large redshift range (up to $z \sim 2.5$); the N2 vs. metallicity relation is monotonic; the $[N II]$ and $H\alpha$ lines can be separated in even

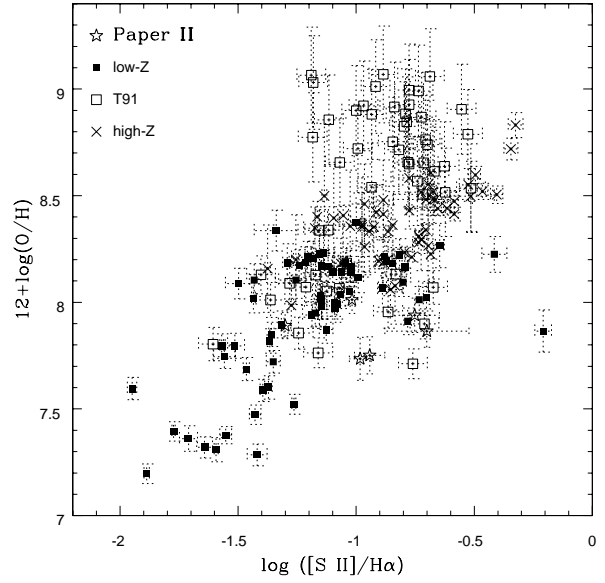


Figure 4. Oxygen abundance versus intensity ratio of the emission lines $[S II] \lambda 6717\text{\AA} + [S II] \lambda 6731\text{\AA}$ over $H\alpha$. The high metallicity sample is from the compilations of Díaz & Pérez-Montero (2000) and Castellanos, Díaz & Terlevich (2001); the low metallicity sample is found in Table 1.

moderate resolution spectra, and the N2 line ratio does not depend on reddening corrections or flux calibration.

On the negative side, N2 is sensitive to ionization and O/N variations implying that, strictly, it should be used mainly as an indicator of galaxy-wide abundances.

Interestingly, the comparison with photoionization models indicates that the observed N2 is consistent with nitrogen being a combination of both primary and secondary origin.

Our main conclusion is that the combination of N2 and S2 provides a tool to roughly map the metallicity of galaxies (and search for low Z galaxies) using survey quality data, like e.g. that of the Sloan Digital Survey, for redshifts in excess of 0.2.

ACKNOWLEDGMENTS

We are grateful to Marcelo Castellanos and Angeles Díaz for providing us data prior to publication. GD would like to thank CNPq-Brazil for a research scholarship, and INAOE for hospitality during a visit to Mexico where part of this paper was written. ET acknowledges support through a research grant from CONACYT-Mexico and everlasting hospitality of IoA.

REFERENCES

- Baldwin J.A., Phillips M.M. & Terlevich, R., 1981, PASP, 93, 5
 Campbell A., Terlevich R. & Melnick J., 1986, MNRAS, 223, 811
 Castellanos M., Díaz A.I. & Terlevich, E., 2001, MNRAS, in press (CDT01)
 Copetti, M. V. F., Pastoriza, M. G. & Dottori, H. A. 1986, A&A, 156, 243

- Díaz A.I., Terlevich E., Vílchez J.M., Pagel B.E.J., Edmunds M.G., 1991, MNRAS, 253, 245
- Díaz A.I. & Pérez-Montero E., 2000, MNRAS, 312, 130 (DP00)
- Dopita M.A., Evans I.N., 1986, ApJ, 307, 431
- Edmunds M.G., Pagel B.E.J., 1984, MNRAS, 211, 507
- Ferland, G.J. 1996, HAZY, a Brief Introduction to Cloudy (Univ. Kentucky Phys.Astron.Dept.Internal Rep.)
- Garnett D.R., 1989, ApJ, 345, 282
- Garnett D.R., 1990, ApJ, 363, 142
- Garnett D.R., Shields G.A., Skillman E.D., Sagan S.P., Dufour R.J., 1997, ApJ, 489, 63
- González-Delgado R.M. *et al.*, 1994, ApJ, 437, 239
- Henry, R. B. C., Edmunds, M. G. & Köppen, J., 2000, ApJ, 541, 660
- Izotov Y.I., Thuan T.X. & Lipovetsky V.A., 1994, ApJ, 435, 647
- Kennicutt R.C., Garnett D.R., 1996, ApJ, 456, 504
- Kniazev A.Y., Pustilnik S.A., Masegosa J., Márquez I., Ugryumov A.V., Martin J.M., Izotov Y.I., Engels D., Brosch N., Hopp U., Merlino S., Lipovetsky V.A., 2000, A&A, 357, 101
- Kobulnicky H.A. & Skillman E.D., 1996, ApJ, 471, 211
- Kobulnicky H.A., Kennicutt R.C. & Pizagno J.L., 1999, ApJ, 514, 544
- Kunth D. & Joubert M., 1985, A&A, 142, 411
- Leitherer, C. & Heckman, T. M. 1995, ApJS, 96, 9
- Lipovetsky V.A., Chaffee F.H., Izotov Y.I., Foltz C.B., Kniazev A.Y., Hopp U., 1999, ApJ, 519, 177
- Mathis J.S., Chu Y.-H. & Peterson D.E., 1985, 292, 155
- McCall M.L., Rybski P.M., Shields G.A., 1985, ApJS, 57, 1
- McGaugh S.S., 1991, ApJ, 380, 140
- Oey M.S. & Shields J.C., 2000, ApJ, 539, 687
- Osterbrock D.E., 1989, Astrophysics of Gaseous Nebulae and Active Galactic Nuclei, Mill Valley: University Science Books
- Pagel B.E.J., Edmunds M.G., Blackwell D.E., Chun M.S. & Smith G., 1979, MNRAS, 189, 95
- Pagel B.E.J., Edmunds M.G. & Smith G., 1980, MNRAS, 193, 219
- Pagel B.E.J., Simonson E.A., Terlevich R.J. & Edmunds M.G., 1992, MNRAS, 255, 325
- Pastoriza M.G., Dottori H.A., Terlevich E., Terlevich R., Díaz A.I., 1993, MNRAS, 260, 177
- Raimann D., Storchi-Bergmann T., Bica E., Melnick J., Schmitt H., 2000, MNRAS, 316, 559
- Ratcliffe A., Shanks T., Parker Q.A., Broadbent A., Watson F.G., Oates A.P., Collins C.A., Fong R., 1998, MNRAS, 300, 417
- Rego M., Cordero-Gracia M., Gallego J. & Zamorano J., 1998, A&A, 330, 435
- Shields G.A. & Searle L., 1978, ApJ, 222, 281
- Skillman E.D., Terlevich R.J., Kennicutt, R.C., Garnett D.R., Terlevich E., 1994, ApJ, 431, 172
- Skillman E.D. & Kennicutt, R.C., 1993, ApJ, 411, 655
- Storchi-Bergmann T., Calzetti D., & Kinney A.L., 1994, ApJ, 429, 572
- Storchi-Bergmann T., Schmitt H., Calzetti D., & Kinney A.L., 1998, 115, 909
- Terlevich E., Terlevich R., Denicoló, G. & Ratcliffe, A., 2001, in preparation (Paper II)
- Terlevich R., Melnick J., Masegosa J., Moles M., Copetti M.V.F., 1991, A&A, 91, 285 (T91)
- Thuan T.X., Izotov Y.I., Lipovetsky V.A., 1995, ApJ, 445, 108
- Torres-Peimbert S., Peimbert M., Fierro J., 1989, ApJ, 345, 186
- van Zee L., 2000, ApJ, 543, L31
- Vílchez J.M., Pagel B.E.J., Díaz A.I., Terlevich E., Edmunds M.G., 1988, MNRAS, 235, 633
- Vílchez J.M. & Esteban C., 1996, MNRAS, 280, 720
- Walsh J.R. & Roy J.-R., 1989, MNRAS, 239, 297